Chemosphere 350 (2024) 141078

Contents lists available at ScienceDirect

Chemosphere

journal homepage: www.elsevier.com/locate/chemosphere

Organic micropollutant removal and phosphate recovery by polyelectrolyte multilayer membranes: Impact of buildup interactions

Akhil Gopalakrishnan [a,1,#], Disha V. Janardhanan [a,2,#], Subha Sasi [a,3], Charuvila T. Aravindakumar [b,c], Usha K. Aravind [a,d,*]

[a] Advanced Centre of Environment Studies and Sustainable Development, Mahatma Gandhi University, Kottayam, India
[b] School of Environmental Sciences, Mahatma Gandhi University, Kottayam, India
[c] Inter University Instrumentation Centre, Mahatma Gandhi University, Kottayam, India
[d] School of Environmental Studies, Cochin University of Science and Technology, Kochi-682022, Kerala, India

HIGHLIGHTS

- At pH 6, PEI/PSS multilayer buildup is based on electrostatic interactions
- At pH 10, PEI/PSS multilayer buildup is based on non-electrostatic interactions
- PEI/PSS assembled at pH 6 favors phosphate recovery
- PEI/PSS assembled at pH 10 favors oxybenzone retention by hydrophobic interactions

GRAPHICAL ABSTRACT

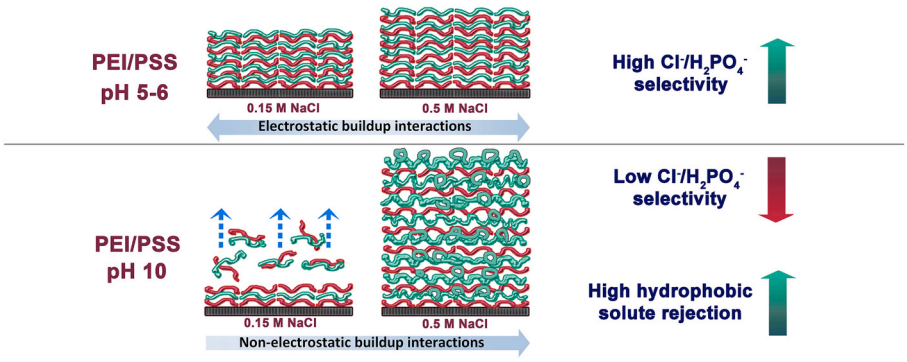

ARTICLE INFO

Handling Editor: Charuvila T Aravindakumar

Keywords:
Layer-by-layer (LbL)
Non-electrostatic
Chloride
Phosphate
UV-Filter
Micropollutant

ABSTRACT

Polyelectrolyte multilayer (PEM) deposition conditions can favorably or adversely affect the membrane filtration performance of various pollutants. Although pH and ionic strength have been proven to alter the characteristics of PEM, their role in determining the buildup interactions that control filtration efficacy has not yet been conclusively proved. A PEM constructed using electrostatic or non-electrostatic interactions from controlled deposition of a weak polyelectrolyte could retain both charged and uncharged pollutants from water. The fundamental relationship between polyelectrolyte charge density, PEM buildup interaction, and filtration performance was explored using a weak-strong electrolyte pair consisting of branching poly (ethyleneimine) and poly (styrene sulfonate) (PSS) across pH ranges of 4–10 and NaCl concentrations of 0 M–0.5 M. PEI/PSS multilayers at acidic pH were dominated by electrostatic interactions, which favored the selective removal of a

* Corresponding author. Advanced Centre of Environment Studies and Sustainable Development, Mahatma Gandhi University, Kottayam, India.
E-mail address: uka@cusat.ac.in (U.K. Aravind).
# These authors contributed equally to this work.
[1] Karlsruhe Institute of Technology, Eggenstein-Leopoldshafen 76344, Germany.
[2] Department of Chemistry, Henry Baker College, Melukavu, 686652, India.
[3] Department of Botany, NSS Hindu College, Changanacherry, 686102, India.

https://doi.org/10.1016/j.chemosphere.2023.141078
Received 26 April 2023; Received in revised form 2 October 2023; Accepted 28 December 2023
Available online 29 December 2023

charged solute, phosphate over chloride, while at alkaline pH, non-electrostatic interactions dominated, which favored the removal of oxybenzone (OXY), a neutral hydrophobic solute. The key factor determining these interactions was the charge density of PEI, which is controlled by pH and ionic strength of the deposition solutions. These findings indicate that the control of buildup interactions can largely influence the physico-chemical and transport characteristics of PEM membranes.

Author statement

Dr. Akhil Gopalakrishnan, Writing - original draft; Investigation; Formal analysis; Data curation; Validation; Software; Visualization; Conceptualization; Writing - review & editing, Disha V Janardhana, Writing - review & editing, Investigation; Formal analysis; Conceptualization; Data curation; Validation;, Subha Sasi, Investigation; Formal analysis; Writing - review & editing, Charuvila T. Aravindakumar, Project administration; Resources; Writing - review & editing, Usha K. Aravind, Funding acquisition; Project administration; Resources; Conceptualization; Writing - review & editing; Data curation; Validation, *CRediT roles as per Elsevier guidelines.

1. Introduction

The widespread occurrence of organic micropollutants (MPs) is a serious issue for the water industry (Luo et al., 2014; Khanzada et al., 2020; Sasi et al., 2020; Enault et al., 2023). The removal of micropollutants using advanced membrane technology gained considerable attention in the past two decades due to the efficient removal of several MPs from water using reverse osmosis (RO), nanofiltration (NF), and ultra-filtration (UF) (Khanzada et al., 2020; Devaisy et al., 2022). NF and RO exhibit good removal of micropollutants whereas UF exhibits poor removal (Khanzada et al., 2020; Devaisy et al., 2022). The high-performance NF uses thin-film-composite membranes (TFC) composed of a thin selective barrier layer synthesized by interfacial polymerization on porous support (Yang et al., 2019). However, the performance of TFC membranes is limited by trade-offs between water permeability and solute selectivity, and high operational pressure. One way to overcome this limitation is to customize the functional layer properties such as the thickness and structure (Zhang et al., 2020). Several mechanisms such as electrostatic interaction, hydrophobic interaction and size exclusion are involved in the removal of MPs depending on their molecular weight (MW), shape, acid dissociation constant (pKa), hydrophobicity (log Kow), and diffusion coefficient (Bellona et al., 2004; Ojajuni et al., 2015). Thus, a functional layer with tunable charge, pore size and hydrophobicity can control the retention of micropollutants.

The surface modification of membranes by polyelectrolyte multilayers (PEMs) using layer-by-layer (LbL) assembly has gained enormous attention due to its versatility and potential in modifying the active layer of membranes for filtration applications (Joseph et al., 2014; Durmaz et al., 2021). When compared to other surface modification methods, the LbL method is a simple, scalable, green and environmentally friendly technique with high functionality, making it ideal for the selective separation of micropollutants and ions (Zhang et al., 2019; Bóna et al., 2023). PEM membranes exhibit high ion separation and outstanding monovalent/divalent ion selectivity (Ouyang et al., 2008; Disha et al., 2012; Cheng et al., 2018; Dong et al., 2022). The high ion retention by PEM is mainly explained by Donnan exclusion and steric hindrance (Cheng et al., 2018; Chen et al., 2023). Interestingly, some PEM can also exhibit high MP retention and monovalent ion/MP selectivity, unlike commercially available NF membranes that retain both ions and MPs simultaneously (Abtahi et al., 2018; Thomas et al., 2020; Athullya et al., 2022). PEM of various compositions is demonstrated to retain organic solutes such as sugars, proteins, amino acids, pharmaceuticals and dyes (Hong et al., 2006; Aravind et al., 2007; Gopalakrishnan et al., 2015; Mathew et al., 2017; Abtahi et al., 2018). In addition to the Donnan exclusion and steric hindrance, the affinity of the MPs to the membrane also plays a role in the removal of MPs by adsorption. Hydrophobic interaction between the membrane and the solute becomes significant especially when the MP is neutral or weakly charged (Abtahi et al., 2018).

The fine-tuning of the multilayer thin film architecture to bring about electrostatic or non-electrostatic effects to confer specific properties such as selectivity towards a micropollutant is quite intriguing. Manipulation of topographical textures, wettability, surface area, and functionality of membranes by PEM helps to formulate customized surface characteristics for water treatment (Joseph et al., 2014; Sanyal and Lee, 2014; Saqib and Aljundi, 2016; Ghiorghita and Mihai, 2021). The buildup parameters during the multilayer deposition determine the properties of a PEM film. For multilayers involving weak and strong polyelectrolyte (PE) combinations, the pH and ionic strength of the deposition solutions could be used as tools for tuning the interactions between the PEs and the physical properties of PEM (Lösche et al., 1998; Sukhorukov et al., 2001; Tiourina et al., 2001; Itano et al., 2005). Multiple interactions between the PEs can function independently or they can co-exist depending on the nature of PEs and deposition conditions. Although the electrostatic interactions between oppositely charged PEs are identified as the most prominent mechanism for PEM buildup in the literature, the PE association induced by secondary interactions such as hydrophobic forces or hydrogen bonding are also demonstrated to result in PEM formation (Kotov, 1999; Zhao et al., 2013; Mohamad et al., 2019). Some early studies on liquid crystalline ionomers revealed that multilayers can be built from polyelectrolytes of very little charge density (Cochin et al., 1997). Thus, it was identified that the electrostatic driving force is not always responsible for the PEM formation. Thermodynamic simulation studies suggest that the entropically driven PEM formation as a result of counterion release is the major mechanism in the strong polyelectrolyte regime, whereas the enthalpically driven mechanism is prominent in the weak polyelectrolyte regime (Ou and Muthukumar, 2006; Rathee et al., 2018). In the case of poor electrostatic interactions of weakly charged polyelectrolytes, loosely bound polyelectrolyte counterions make PEM formation more enthalpically favourable (Rathee et al., 2018). However, the argument that the 'free energy of PEM formation can be enthalpically favourable for a weakly charged polyelectrolyte' is not supported by sufficient experimental evidence perhaps due to the challenges in measuring minuscule heat changes involved in PEM formation. The advent of sensitive calorimetric instrumentation has recently helped to identify the rise in entropy as the main driving force for the PEM buildup (Fu and Schlenoff, 2016). There is an increasing agreement among the PEM researchers in accord with the entropy-based concept that counterion release plays a vital role in PEM buildup. The entropy gained during PE association due to the release of the counterions and bound water molecules serves as the driving force even if there is no charge reversion taking place at alternate PE layer deposition (von Klitzing, 2006). Kotov (1999) suggested the contribution of entropy to the LbL assembly mechanism and concluded that the entropy change during PEM buildup is caused by i) the release of counterions from the hydration shell of polyelectrolytes, ii) the reorientation of water molecules associated with charged function groups of PE upon the association of PE, iii) release of water molecules around hydrophobic parts of PEs, and iv) loss of PE chain mobility upon PE association. The release of trapped water molecules may even lead to the reorganization of hydrophobic regions in the PE, thereby promoting hydrophobic interactions (Kotov,

1999). The interaction of hydrophobic domains in PEs may significantly influence the properties of the PEM such as an increase in the thickness of the layers (Guyomard et al., 2005). A stable multilayer can be formed at high ionic strength by the hydrophobic associations of PE which control the release of water leading to a gain in entropy (Schlenoff et al., 2008). Multilayer assemblies formed by hydrophobic interactions have constituted promising platforms for antibacterial surfaces (Lu et al., 2015), bio-electrocatalytic interfaces (Lorena Cortez et al., 2014), tissue engineering substrates (Wang et al., 2005), and permselective coatings (Shchepelina et al., 2011; Zhao et al., 2013).

The inter-polyelectrolyte interaction can shift from electrostatic to water-mediated hydrophobic interaction depending on the pH and ionic strength of the PE solution (Kotov, 1999; Sumi et al., 2009; Ogawa, 2015). The degree of ionization of a weak PE depends on its solution pH. Hence the net charge and the extent of electrostatic interaction of a weak PE can be varied easily by controlling the pH and ionic strength. Polyethyleneimine is a weak polycation mostly used as an anchoring first layer during multilayer deposition (Kolasińska et al., 2007). Branched PEI consist of 1°, 2° and 3° amino groups. 2° amine groups present in the backbone contribute to 50% of the total amine groups whereas 3° amine groups in the backbone and 1° amine groups in the side chain contribute 25% each to the total amine groups (Clark and Hammond, 2000). The 1°, 2°, and 3° amine groups have a wide range of pKa values of 11.6, 6.7 and 4.5 respectively which helps to control the ionization of PEI greatly by changing the solution pH (Willner et al., 1993).

PEI/poly (styrene sulfonate) (PSS) is a versatile weak polycation-strong polyanion system which is not been very much explored for controlling hydrophobic interactions. The PEI/PSS polyion pair is largely used as a precursor layer due to its adhesion properties (Lvov et al., 1995; Kolasińska et al., 2007; Peng et al., 2012). Our previous work (Disha et al., 2012) demonstrated that PEI/PSS multilayer film deposited at pH 6 act as ion exchange membranes with high selectivity towards $Cl^-/H_2PO_4^-$ ion permeation. Phosphorous (P) plays a crucial role in modern agriculture, but its discharge into water bodies, as a result of sewage and industrial effluents and agricultural run-offs promotes eutrophication (Hasan et al., 2021; Pap et al., 2023). The recovery of P from water is therefore beneficial as a nutrient recycling strategy and also as a solution to mitigate phosphate pollution in water (Bogdan et al., 2020; Pap et al., 2023). PEI/PSS multilayers are suitable for phosphate recovery due to the phosphate-multilayer charge interactions and a high affinity of phosphate to PEI (Disha et al., 2012). The change in PEI/PSS assembly conditions from electrostatic to non-electrostatic may well affect the phosphate recovery. However, this may in turn enhance the retention of hydrophobic compounds by PEI/PSS. The removal of pharmaceutically active and endocrine disrupting compounds which mostly constitute such hydrophobic solutes is usually performed by tight, low molecular weight cut-off membranes. Oxybenzone (OXY, benzophenone-3; 2-hydroxy-4-methoxphenyl phenylmethanone; CAS No. 131-57-7) is one of the most widely used UV-filters in sunscreens, the exposure to which may lead to endocrine disruption in vertebrate systems and toxicity in fish, algae, plants and marine mammals (Downs et al., 2022). OXY and other benzophenones have been identified in water sources worldwide and their toxicity has been raising concerns for both humans and aquatic environments (Schneider and Lim, 2019; Gavrila et al., 2023; Scheele et al., 2023). OXY is a neutral hydrophobic compound which is not easily removed by common water treatment techniques in waste water plants (Schneider and Lim, 2019; Katibi et al., 2021). Therefore, developing efficient membranes for the elimination of benzophenones from water is advantageous from both a health and an environmental standpoint.

This work focused on studying PEI/PSS multilayers in two aspects: i) understanding the growth behavior of the multilayer in the strongly ionized region (acidic pH) and weakly ionized region (alkaline pH) at different ionic strengths, ii) application of the PEI/PSS multilayer membrane in the strongly ionized and weakly ionized states for the recovery/removal of suitable ionic/non-ionic pollutants. Monovalent phosphate ions were selected as the model pollutant for filtration through PEI/PSS multilayer formed at pH 6, where electrostatic interactions are dominant. A non-ionic hydrophobic micropollutant OXY was selected as a model pollutant for filtration through PEI/PSS multilayer formed at pH 10 where hydrophobic interactions are dominant. The ionic strength is varied from 0 to 0.5 M NaCl to examine the effect of doping and charge screening on polyelectrolyte association. The pH and salt-driven shift in buildup interactions of PEI and PSS from electrostatic to non-electrostatic is found to affect the internal structure, surface properties, ion transport selectivity and rejection of a model hydrophobic micropollutant OXY. The separation window of the membrane towards the selective transport of anions is considerably reduced by switching the deposition conditions in favour of non-electrostatic buildup interaction. However, at a low ionized state of PEI, multilayers of large thickness are grown using hydrophobic interactions that favors the removal of OXY. These results illustrate that the switching of electrostatic and non-electrostatic interactions could be used for the selective removal of hydrophobic emerging contaminants and phosphate recovery from water. The low pressure filtration membranes put forth in this study could be used as pre-filters for NF/RO systems used to treat municipal waste water or small-scale domestic wastewater. Such pre-filters are expected to reduce the load on the NF/RO systems, increase the life of the membrane modules, and minimize the discharge of phosphate and sunscreens into the waters bodies.

2. Experimental

2.1. Materials

Nylon 6, 6 (0.45 μm pore size, Pall Life Sciences) membranes were used as support for LbL-modified membranes used in filtration. Silicon wafers of [100] orientation, polished on one side was used as supports for multilayer deposition for ellipsometry measurements. PVDF (0.2 μm pore size, Millipore) and Nylon 6, 6 membranes were used as supports for contact angle measurements. Poly (styrene sulfonate) (PSS, M_w = 70,000 Da, 30 wt% aqueous solution), branched poly (ethyleneimine) (PEI, M_w = 750,000 Da, 50 wt % aqueous solution), oxybenzone (OXY) and NaCl from Sigma Aldrich, and sodium dodecyl sulphate (SDS), NaH_2PO_4, HCl, and NaOH from Merck were used as received. Ultrapure water of resistivity 18.2 MΩcm was used for the multilayer buildup and permeation experiments.

2.2. Deposition of polyelectrolyte multilayers

The commercial supporting membranes were rinsed and stored in ultrapure water for at least 15 h before modification. The LbL assembly was carried out by the alternate immersion of the supporting membrane in the solutions of the cationic polyelectrolyte (PEI, 0.02 M) and the anionic polyelectrolyte (PSS, 0.02 M) for 15 min each. Each immersion step involved intermittent washing steps with ultrapure water (pH 6.0 ± 0.5). Immersion and washing cycles were repeated to get the required number of layers. Each immersion step was limited to 15 min. A PEM is represented as '$(PEI/PSS)_x$' or 'x bl' where x is the number of layer pairs (bilayer). The pH of polyelectrolyte solutions was adjusted in the range 4–10 with 1 M HCl and NaOH. The ionic strength of the polyelectrolyte solutions was controlled by adjusting the NaCl concentrations in the range 0–0.5 M. The pH of 4–10 and NaCl concentration 0–0.5 M were chosen to ensure observable changes in the PEI/PSS charge density based on the aqueous environment without destabilizing the multilayer structure.

2.3. Characterization of polyelectrolyte multilayers

PEM buildup was analyzed by Fourier-transform infrared (FTIR) spectrophotometer (Shimadzu IR Prestige-21). The IR spectra were recorded in absorbance mode from 650 to 4000 cm^{-1} using ZnSe

attenuated total reflectance (ATR) attachment. The number of scans per spectrum was 20 and the resolution was 4 cm^{-1}. The thickness of the multilayers deposited on silicon wafers was evaluated using a spectroscopic ellipsometer (M − 2000V, J.A. Woollam Co.) in the wavelength range 370–1000 nm. The measurements were made by following the protocol reported previously (Gopalakrishnan et al., 2015). Surface morphologies of membranes were recorded by scanning electron microscope (SEM, JEOL- JSM-6390). Samples were sputter coated with platinum using a JEOL JFC-1600 autofine coater. Atomic force microscopy (AFM) in non-contact mode was used to evaluate the topography, phase and roughness of membranes using a Witec alpha 300 RA (force constant 42 N m^{-1}, resonance frequency 285 kHz). Images of the surfaces obtained from 10 μm × 10 μm scans were used for the root mean square roughness (Sq) analysis. Image corrections such as third-order polynomial background subtraction and plane levelling using Witec Project Plus and Gwyddion 2.42 software were performed before roughness analysis. The profile of water drops on the PEM surface for contact angle measurement was analyzed using images captured with a high-resolution video camera. Images were then processed with ImageJ software using a contact angle plug-in. Reported contact angle values are the average of five parallel measurements and are reported as mean ± standard deviation. A detailed description of measurements is provided in section 2 of Supporting Information.

2.4. Transport studies

Filtration experiments were performed in an Amicon-8050 dead-end stirred cell with a 50 mL capacity and an effective membrane area of 13.4 cm^2. N_2 pressure of 0.3 ± 0.1 bar at the pressure gauge at a stirring speed 400 rpm was maintained during filtration. For ion permeability studies, a synthetic feed solution was prepared by mixing NaCl and NaH_2PO_4 at 100 ppm concentration. Micropollutant filtration was carried out using 10 mg/L solutions of OXY in ultrapure water. To study the effect of anions on OXY removal, sodium salts of Cl^-, SO_4^{2-}, and NO_3^- were added separately to the OXY solution and stirred well for 3 h to get a final anion concentration of 50 mg/L. For the filtrations involving surfactant, 8.2 mM SDS tock solutions were prepared corresponding to 1 CMC. 0.5 and 0.05 CMC solutions were prepared from this stock solution and OXY was added and stirred for 12 h to get a final OXY concentration of 10 mg/L. The pH of all feed solutions were adjusted to 6.5 ± 0.5. 25 mL of OXY 25 mL of micropollutant feed was used for each cycle of batch filtration. Ion concentrations were analyzed using a Dionex 1100 ion chromatograph with An Ionopac AS12A column and a conductivity detector. 2.7 mM Na_2CO_3/1.0 mM $NaHCO_3$ was used as eluent at a flow rate of 1.0 mL/min. The concentration of OXY in the feed and permeate was monitored using High-Performance Liquid Chromatography (Shimadzu prominence UFLC, LC 20AD) connected with a diode array detector (SPD-M20 A) and an Enable C18G 250 mm × 4.6 mm × 5 μm column. The mobile phase consisted of acetonitrile and water in 30:70 ratios. The flux, percent rejection, and selectivity were calculated using equations (Disha et al., 2012) given below:

Flux was calculated using Equation (1) where V is the volume (L) of permeate collected, A is the effective membrane area (m^2) and Δt is the permeation time (h).

$$\mathbf{J} = \frac{V}{A \bullet \Delta t} \tag{1}$$

The percentage rejection (R (%)) was calculated using Equation (2) where c_{feed} and c_{perm} are the concentrations of the feed and permeate respectively.

$$\mathbf{R}(\%) = \frac{c_{feed} - c_{perm}}{c_{feed}} \bullet 100 \tag{2}$$

The selectivity (α_s) was calculated using Equation (3) where c_A and c_B are concentrations (mg/L); and R_A and R_B are the percentage rejections of components A and B respectively.

$$\propto_s = \frac{c_{A_{perm}} \bullet c_{B_{feed}}}{c_{A_{feed}} \bullet c_{B_{perm}}} \text{ Or } \propto_s = \frac{100 - R_A}{100 - R_B} \tag{3}$$

3. Results and discussion

3.1. The role of buildup conditions on the properties of LbL-assembled membranes

The multilayers are constructed from PEI and PSS on polyamide MF membranes at various deposition pHs. To manipulate the amount of available charged sites of both PEI and PSS, the ionic strength of the assembly solutions is also varied at selected deposition pH. As the polycation- PEI has three different ionizable amino groups, the degree of ionization can be varied to a large extent by selecting a suitable assembly pH. The polyelectrolyte deposition pH is set in the range 4–10 and the deposition ionic strength is set in the range 0–0.5 M NaCl.

3.1.1. PEM growth trends at varying buildup pH and ionic strength

PEI/PSS multilayer buildup as a function of pH and ionic strength is observed from the sulfonate group peak of PSS at 1033 cm^{-1} in ATR-FTIR spectra (Fig. 1a). The area under the sulfonate peak is found to grow with the increase in deposition pH in both 0 and 0.5 M NaCl ionic strengths. The highest amount of adsorbed polyelectrolyte is observed for pH 10 at 0.5 M NaCl.

SEM images (Fig. 1b) reveal that the surface deposition of multilayers is very dense and the surface porosity is reduced at higher pHs. The connectivity and surface coverage of multilayers is also maximum when deposited from polyelectrolyte solutions of pH 10 and 0.5 M NaCl. In the absence of salt, an increase in the mass deposition with the increase in pH is observed in the SEM images (Fig. S2) and in spectroscopic ellipsometry thickness (Fig. 2). $(PEI/PSS)_8$ deposited at pH 6 without NaCl shows a thickness of 7 nm which increases to 37 nm in the presence of 0.5 M NaCl, in agreement with the reported value in the literature (Elzbieciak et al., 2009). $(PEI/PSS)_8$ deposited at pH 10 shows a thickness of 13 and 76 nm when deposited without NaCl and with 0.5 M NaCl respectively. Both pH and ionic strength of solutions affect the deposition of the weak polycation and the strong polyanion as expected.

pH can regulate charge density along weak polyelectrolyte chains thus inducing their conformational changes and mutual interactions (Decher and Schlenoff, 2003). Thus, in the absence of salt, the coiling of the weakly charged PEI should be responsible for the increased thickness of the film at pH 10. When deposited from solutions containing salt (eg. 0.5 M NaCl as in the present case), the adsorbed amount of polyelectrolytes per unit area increases due to conformational changes in the polyelectrolyte as a result of charge screening (Lösche et al., 1998; Ruths et al., 2000; Shiratori and Rubner, 2000). It is interesting to note that the multilayer growth follows pH-dependent exponential curve (Fig. 2) on moving from pH 6 (where PEI is strongly charged), to pH 10 (where it is weakly charged). It can be deduced from Figs. 1 and 2 that at pH 10, high buildup of the multilayer occurs, where the degree of ionization is low (see Table S1) for PEI and its electrostatic interaction is poor. At pH 6, PEI is more than 50% ionized whereas, at pH 10, it is only about 5% ionized. Considering the pKa values of 1° (~11.6), 2° (~6.7), and 3° (~4.5) amine groups (Willner et al., 1993), only the 1° amine groups are expected to be protonated at pH 10. Yet, the influence of added salt on the increase in the amount of adsorbed polyelectrolyte is apparent at both low and high ionized states of PEI.

3.1.2. Anomalous growth trend at two different buildup salt concentrations

Generally, an increase in ionic strength initially leads to a regular increase in film thickness (Dubas and Schlenoff, 1999; Guzmán et al., 2009) up to a certain ionic strength (typically in the range of 1–2 M NaCl) and destabilizes the PEM at very high ionic strengths (von Klitzing, 2006; Chen et al., 2023). To evaluate the effect of salt concentration on PEM buildup, PEI/PSS multilayer deposition was monitored at a salt

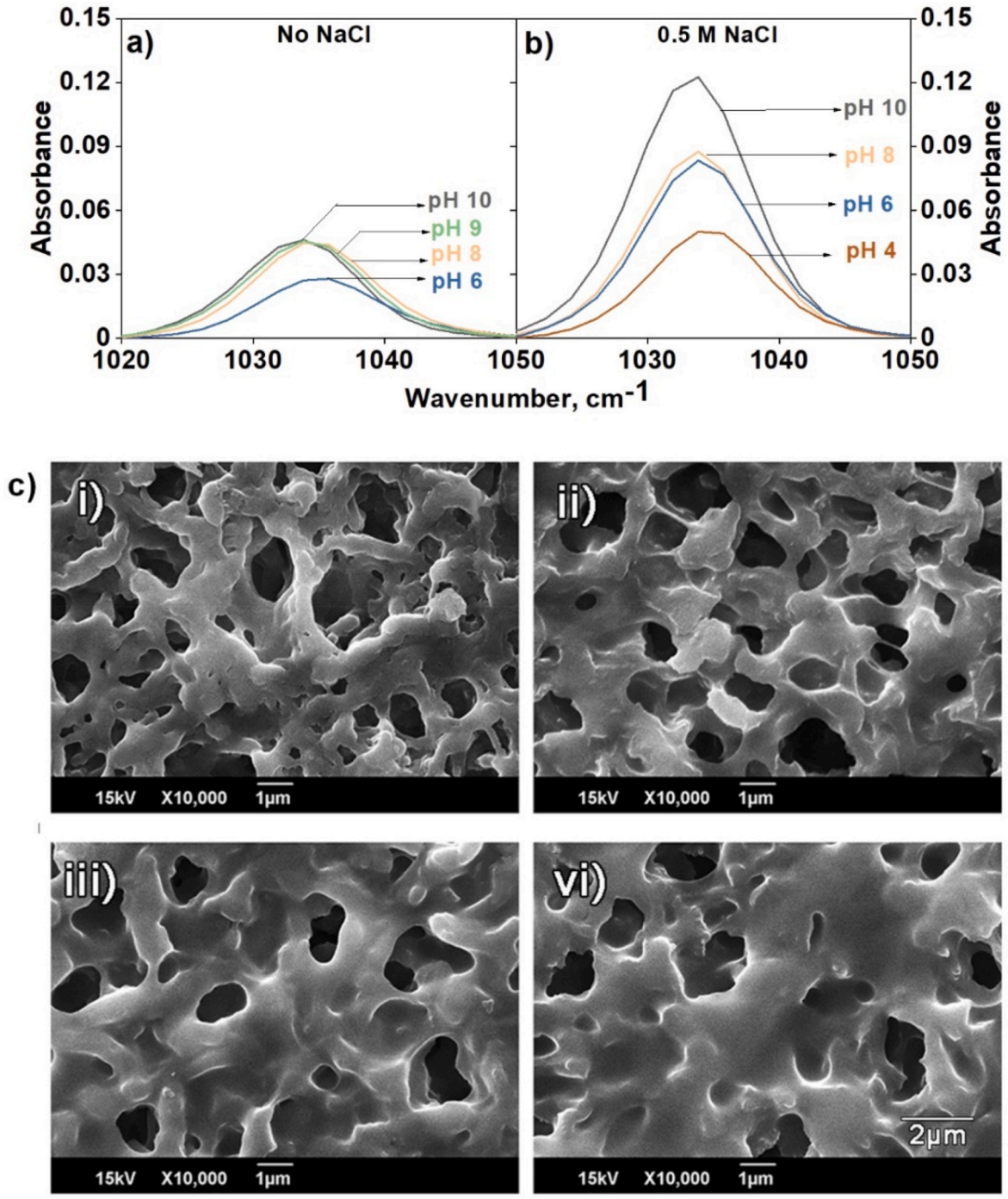

Fig. 1. PEI/PSS multilayer buildup as a function of polyelectrolyte solution pH and salt: ATR-FTIR spectra of $(PEI/PSS)_7$ (a) without salt, and (b) with 0.5 M NaCl. (c) SEM images of $(PEI/PSS)_9$ on nylon support at pH (i) 4 (ii) 5.9 (iii) 8 and (vi) 10 deposited from 0.5 M NaCl solutions.

concentration of 0.15 M NaCl and the results were compared with that of 0.5 M NaCl at different deposition pH. At 0.15 M NaCl, the amount of polyelectrolyte deposited increased slightly with a pH change from 6 to 8 and then decreased abruptly with a pH change from 8 to 9 and 10, contrary to that of 0.5 M NaCl (Fig. 3). A corresponding less denser layer formation is visible in SEM images of $(PEI/PSS)_7$, as pH is changed from 8 to 9 (Fig. S3).

The deposition of PEI/PSS multilayer film at 0.15 and 0.5 M salt concentrations shows that multilayer film growth need not produce regular thickness increments at all salt concentrations. The deposition of PEI/PSS from solutions of pH 6 and various ionic strengths was explained previously (Disha et al., 2012) based on electrostatic forces. However, the explanation based on electrostatic interaction does not perfectly match when thick film deposition takes place at a low ionized state of PEI at a high salt concentration (0.5 M) and thinner deposition takes place at a low salt concentration (0.15 M). This leads to the hypothesis that non-electrostatic interactions are possibly involved in PEI/PSS multilayer buildup at low ionized states of PEI (alkaline pH). According to the electrostatic model, the electrostatic interactions determined by the ionization and charge density of the polyelectrolytes act as a driving force for multilayer formation. However, the current understanding of the PEM buildup underlines that electrostatic attraction by the charge reversal is not a fundamental criterion for multilayer formation (Fu and Schlenoff, 2016; Guzmán et al., 2020).

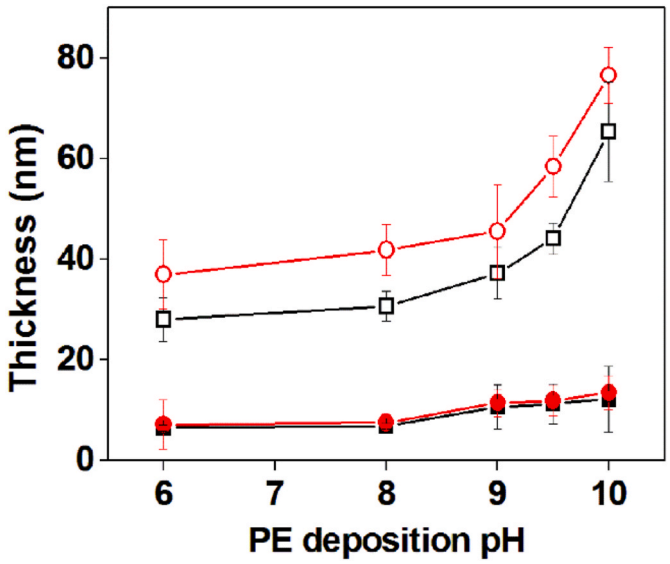

Fig. 2. Ellipsometric thickness of $(PEI/PSS)_7$ (square) and $(PEI/PSS)_8$ (circle) deposited on Si wafers for deposition pH 6–10. Closed symbols represent films adsorbed from solutions without salt and open symbols represent those with 0.5 M NaCl.

Non-electrostatic interactions, also known as secondary interactions could play a significant role in PEM buildup. The coiled structure of PEI and the styrene backbone of PSS can deliver an environment for hydrophobic interactions (Nestler et al., 2012). The hydrophobic interaction of the PE chains is supported by the entropy gain upon the liberation of water molecules associated with polyelectrolytes. Due to the contribution to entropy, the buildup at the hydrophobic regime is a thermodynamically feasible process (Kotov, 1999). It is fairly convincing that hydrophobic interaction is the key driving mechanism for the PEM buildup at pH 10. Interestingly, the hydrophobic interactions could bring about a negative shift (Choi and Rubner, 2005) in the pKa value of PEI which in turn contributes to some extent of electrostatic interaction due to weak ionization. It can be proposed that at basic deposition pH, hydrophobic interaction between the backbones of PEI and PSS and a very weak electrostatic interaction between their functional groups are holding the multilayers together.

3.1.3. Buildup interactions responsible for the effect of salt at low and high ionized states of PEI

The polyelectrolyte deposition from solutions of pH 6 and pH 10 was further analyzed at intermediate salt concentrations. The corresponding results are given in Fig. 4. An unusual deposition trend is observed when ionic strength is increased from 0.05 to 0.5 M NaCl. At pH 10, a fall in the amount of polyelectrolyte deposited was observed initially on adding 0.05 M NaCl which was followed by an increase in mass deposited for each increment in added salt. Above 0.3 M NaCl, the amount of polyelectrolyte deposited was found to be much higher at pH 10 when compared with pH 6 which was not expected if one considers electrostatic interaction alone. The pH and salt-dependent growth patterns of 7 and 8 bilayers are shown in detail using ATR-FTIR spectra (Fig. S5 and Fig. S6).

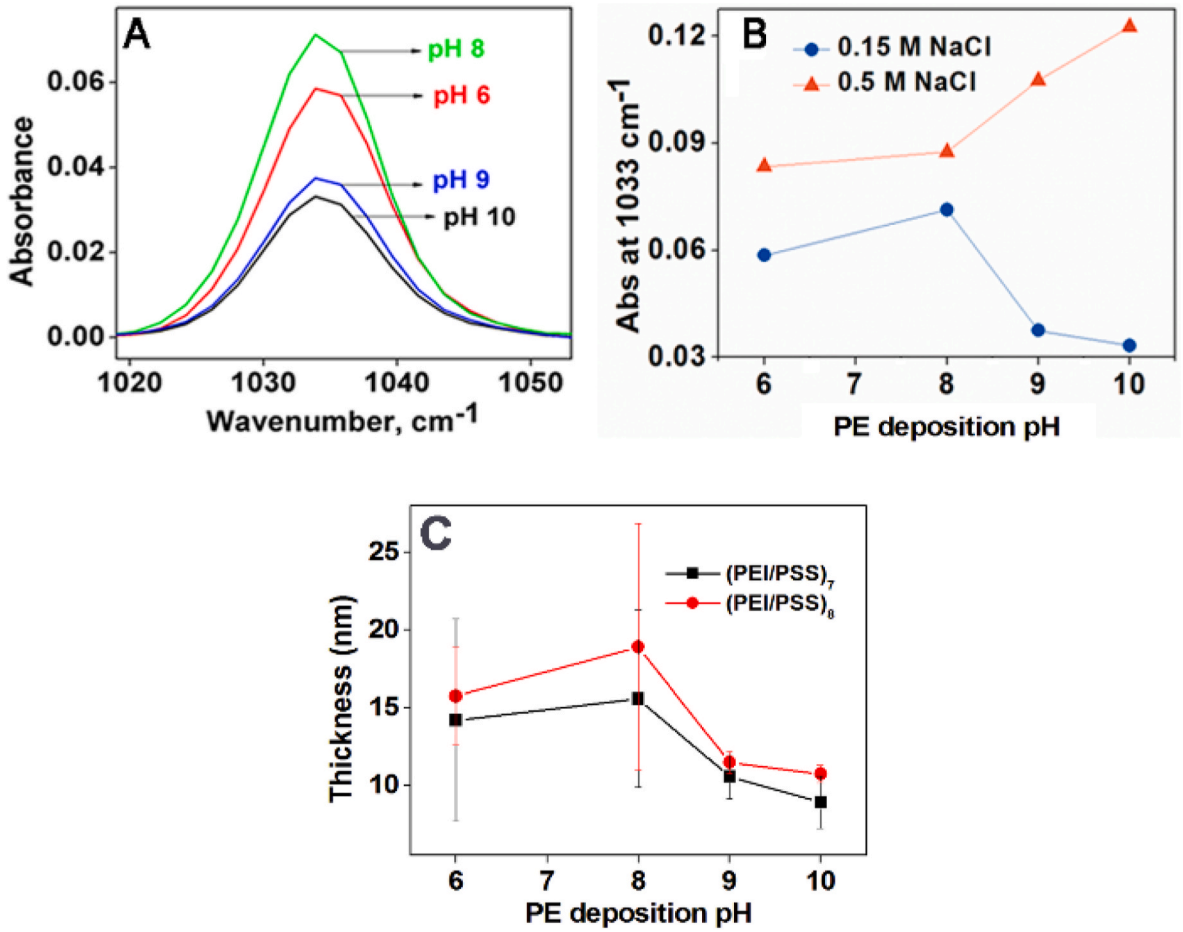

Fig. 3. PEI/PSS multilayer deposition as a function of pH: (A) ATR-FTIR spectra of $(PEI/PSS)_7$ deposited at 0.15 M NaCl, (B) PSS intensity of $(PEI/PSS)_7$ deposited at 0.15 M and 0.5 M NaCl in terms of SO_3^- peak absorbance at 1033 cm^{-1} (C) Ellipsometric thickness of $(PEI/PSS)_7$ and $(PEI/PSS)_8$ films deposited at 0.15 M NaCl.

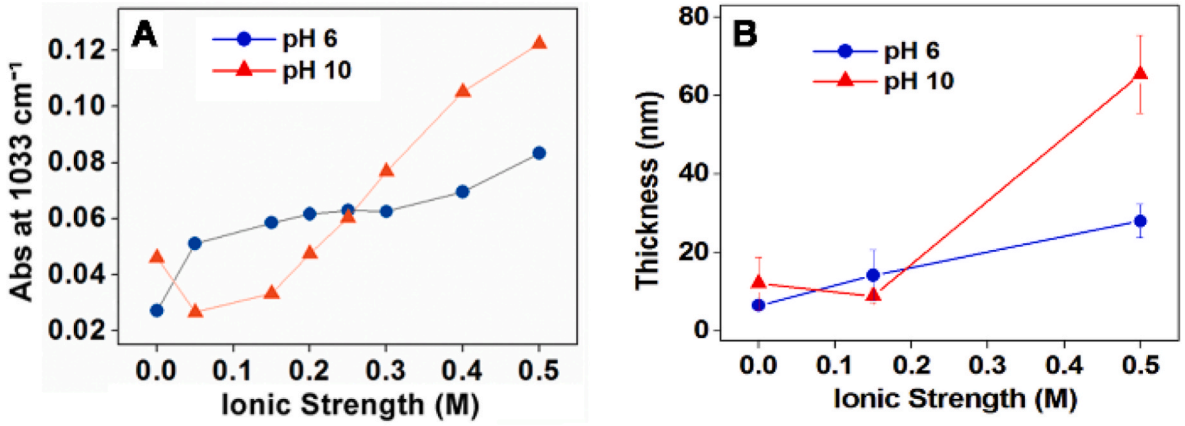

Fig. 4. Film growth of $(PEI/PSS)_7$ for polyelectrolyte solution at deposition pHs 6 and 10 at an ionic strength of 0–0.5 M NaCl: (A) FTIR intensity of the sulfonate peak at 1033 cm^{-1} and (B) Ellipsometric thickness.

The addition of 0.05 and 0.15 M NaCl into the polyelectrolyte deposition solution leads to a thinner multilayer formation at pH 10. This characteristic is in close agreement with the previous report (Elzbieciak et al., 2009). This behavior of low PEM deposition at pH 10 and low salt can be explained based on both electrostatic and thermodynamic models. The polyelectrolytes deposited from solutions containing 0.15 M NaCl are aggregated as loosely bound polyelectrolyte complexes (PEC) (Kovacevic et al., 2002; Schoeler et al., 2002) which can be observed in SEM (Fig. S4). The previous reports that support the formation of PEC in similar conditions are summarized under Fig. S4. The loosely bound PEC desorb in the consecutive deposition and washing steps, resulting in a thinner film which is also evident from ellipsometry and FTIR measurements (Fig. 4). The thinner film formation apparently by the removal of mass from the surface is prominent when deposited from solutions of low ionic strength (0.05–0.15 M). Further increment in the salt concentration above 0.2 M NaCl increases the amount of mass adsorbed. The deposition of increased mass with salt is supported by the observation of flux decline values as presented in Table S3. The addition of salt above 0.2 M NaCl concentration gradually reduces electrostatic interactions, but the hydrophobic interaction gains importance.

The extrinsic compensation from salt ions may result in large mobility to polyion chains (Nazaran et al., 2007). The low charge density of PEI at alkaline pH may support its interdiffusion (Zacharia et al., 2007; Wang et al., 2011) from the bulk of the film to the surface when dipped in PSS. This implies more coalescence of associated polyelectrolytes. The coalescence of polyelectrolyte chains creates the proximity of hydrophobic regions. This may enable more uptake of PSS in the PSS dipping step and also contribute to hydrophobic forces when deposited at pH 10. PSS is known to form dense layers on hydrophobic surfaces (Nestler et al., 2012). The contact angle measurements were performed to understand the wettability of multilayer film deposited from polyelectrolyte solutions of pH 6 and 10. Contact angles of the surfaces of $(PEI/PSS)_7$ deposited at different salt concentrations on PVDF substrates were analyzed. When deposited at pH 10, the contact angles were slightly increased from 99 ± 3° to 102 ± 3° on increasing salt concentration from 0 to 0.15 M NaCl. It was reduced to 89 ± 5° and 85 ± 4° when deposited from polyelectrolyte solutions containing 0.5 and 1 M NaCl respectively. On the contrary, the contact angles were found to rise with salt concentration when deposited from polyelectrolyte solutions of pH 6 (Fig. S1). In all the conditions, PEI/PSS multilayers deposited at pH 6 were hydrophilic (contact angle <50°) when compared to the multilayer deposited at pH 10.

The surface features of PEI/PSS multilayer deposited at pH 10 and pH 6 and different salt concentrations were evaluated using AFM in non-contact mode (Fig. 5). The height and phase imaging were performed to gain information on the topography, roughness and stiffness of the multilayer under different ionic strength and pH (see section 4, Supporting Information). $(PEI/PSS)_7$ deposited at pH 6 without NaCl (Fig. 5a) shows spherical nodular topography with the maximum height of a globular domain up to 1.4 μm and a root mean square (RMS) roughness (Sq) of 494 nm. The phase contrast image shows a homogenous phase distribution with moderate stiffness. When the deposition salt was increased to 0.15 M NaCl at pH 6 (Fig. 5b), the topography became smoother (Sq = 303 nm) with the disappearance of globular domains. This is apparently due to the deposition of a larger amount of extrinsically compensated polyelectrolytes. The phase contrast image shows less phase homogeneity and lower stiffness. At 0.5 M NaCl, pH 6 (Fig. 5c) deposited surface is dense with lower porosity, low Sq (266 nm) and uneven phase distribution. Multilayer deposited at pH 10 without salt (Fig. 5d) shows blunt topography with an Sq of 322 nm. The increase in salt concentration to 0.15 M (Fig. 5e) resulted in compact topography with a very low Sq of 267 nm (in accord with observations in Fig. 3C). The phase turned out to be homogeneous and stiffer. At pH 10 and 0.5 M NaCl (Fig. 5f), however, very thick and rough topography was observed with an Sq 757 nm. This is in agreement with the previous observation (Elzbieciak et al., 2009) that a non-monotonous deposition of PEI/PSS takes place at 0.15 M NaCl and pH 10.5. The polyelectrolytes deposited from solutions containing 0.15 M NaCl are aggregated as loosely bound PEC (Kovacevic et al., 2002) and get desorbed.

3.2. $Cl^-/H_2PO_4^-$ permeation characteristics of PEI/PSS films

The PEI/PSS multilayers deposited in the electrostatic interaction domain (acidic deposition pH) and in the hydrophobic interaction domain (basic deposition pH) are expected to show different responses for anion retention. To understand the specific charge effects (Donnan exclusion) of PEI/PSS, the multilayer was deposited on a microfiltration substrate. The resulting composite membrane is microporous (see Fig. S2), thereby ruling out the possibility of size exclusion of anions under study. The anion retention behavior of PEI/PSS films deposited from polyelectrolyte solutions of various pH was studied for mixed ions of chloride and phosphate at a feed pH 6.5 ± 0.5 in low-pressure filtration. The major phosphate species is the monovalent $H_2PO_4^-$ at this pH (Cerozi and Fitzsimmons, 2016). The retention and selectivity of $Cl^-/H_2PO_4^-$ through PEI/PSS multilayer films were monitored for PE deposition pH 4–10 (Table 1). The results are compared with our previous report (Disha et al., 2012) at pH 5.4 in Table 1. The percentage rejection of phosphate increased and that of chloride decreased with the number of bilayers at a given pH. About 98% of phosphate was rejected by $(PEI/PSS)_9$ at the deposition pH 5.4. Whereas the percentage rejection of phosphate remains rather low at pH 10, despite the large amounts of polyelectrolytes deposited at higher ionic strength (as illustrated in

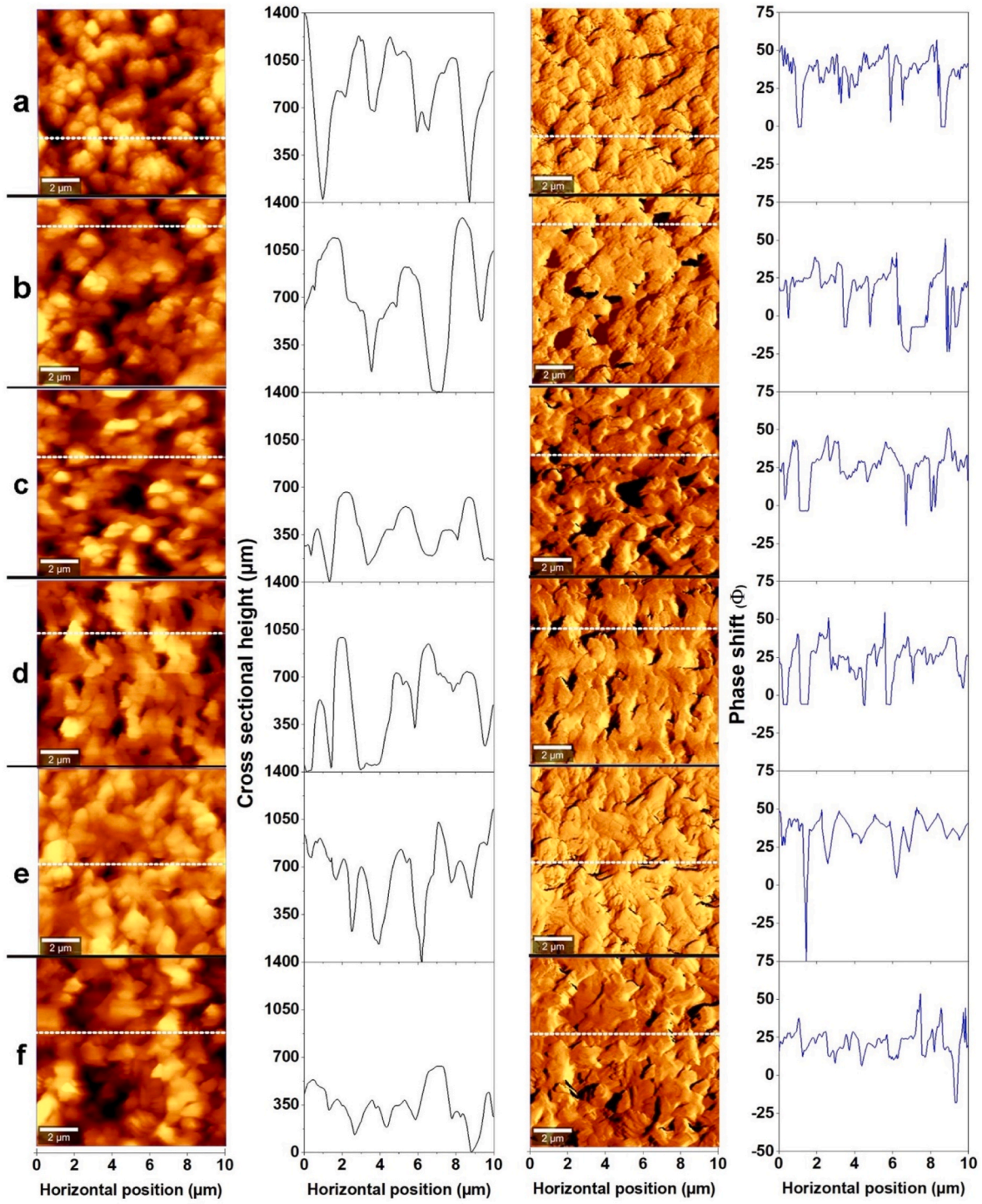

Fig. 5. AFM images of $(PEI/PSS)_7$ deposited at various NaCl concentrations at pH 6: a) no NaCl, b) 0.15 M NaCl and c) 0.5 M NaCl, and at pH 10: d) no NaCl, e) 0.15 M NaCl and f) 0.5 M NaCl. Images from left to right show height image, cross-sectional height, phase contrast image, and cross-sectional phase shift respectively. The cross-sectional data are measured along the horizontal lines marked in the corresponding height and phase contrast images. All AFM images are measured at 10 × 10 μm^2.

Fig. 4). The phosphate rejection is only about 55% at pH 10. The phosphate rejection is reduced by 43% at pH 10 when compared to pH 6 at a deposition salt of 0.5 M NaCl. Chloride ions showed increasing negative rejection with the layer number at all deposition pHs. The decrease in the $Cl^-/H_2PO_4^-$ selectivity is distinct with the increment in deposition pH.

There are three major mechanisms possible for anion removal by the PEI/PSS multilayer membrane: i) charge exclusion (Donnan exclusion) of phosphate by the negatively charged PSS terminating layer on PEI/PSS multilayer, ii) ion exchange of anions with the positively charged amino groups of PEI iii) enhanced binding of phosphate with amino groups of PEI by hydrogen bonding. Donnan exclusion in varying degree may operate in all conditions due to the negative charge of PEI/PSS multilayer (in the range of −30 mV as observed in the previous reports (Shchukin et al., 2006; Guo et al., 2015; Korzhova et al., 2020)) owing to the PSS terminating layer. The ion exchange mechanism can operate on

Table 1
Transport profile of $Cl^-/H_2PO_4^-$ (100 ppm) through PEI/PSS (0.02 M, 0.5 M NaCl) with different deposition pHs and number of bilayers.

pH	Chloride rejection (%)[a]				Phosphate rejection (%)[a]				$Cl^-/H_2PO_4^-$ selectivity[b]			
	6 bl	7 bl	8 bl	9 bl	6 bl	7 bl	8 bl	9 bl	6 bl	7 bl	8 bl	9 bl
4.0	−116	−139	−256	−302	63	84	96	98	6	15	81	245
5.4	−151	−212	−219	−269	70	82	97	99	8	17	93	310
8.0	−109	−122	−130	−179	58	66	70	79	5	7	7	13
10.0	−14	−29	−41	−67	40	44	50	55	2	2	3	4

Note: The negative rejection of Cl-is due to the electric potential difference as a result of the selective retention of a H2PO4- and permeation of Na+.
[a] Error $\leq \pm$ 4%.
[b] Error $\leq \pm$ 6%.

both chloride and phosphate ions with a highly charged PEI/PSS multilayer due to the presence of strongly ionized amino groups of PEI at acidic deposition pH. Whereas the hydrogen bonding mechanism particularly favors phosphate adsorption (Copley and Barton, 1994; Kim et al., 2020, 2022; Xanthopoulou et al., 2021) over chloride on PEI/PSS multilayer even when PEI is in the poorly ionized state (deposited at basic pH) which result in higher retention of phosphate and high $Cl^-/H_2PO_4^-$ selectivity.

The deposition condition around pH 5.4 must be is producing open membranes (highly permeable porous membranes with less denser skin layer) with excess surface charge, and the deposition at pH 10 is producing dense membranes with poor surface charge. At the acidic deposition pH, a synergistic action of Donnan exclusion, ion exchange and hydrogen bonding mechanisms must be highly permeable porous skin with plenty of protonated amino groups of PEI acting as ion exchange sites are responsible for the observed high selectivity (Disha et al., 2012). Towards the basic deposition pH, the degree of protonation of PEI reduces and amino groups become weakly charged. Thus, the mechanism of anion removal is limited to Donnan exclusion and hydrogen bonding. An account of the protonated sites becomes clearer through the examination of the charge density of the backbone of branched PEI. The major share of the overall charge density at a fully ionized state is contributed by the secondary amine group (50%), the rest being primary and tertiary (25% each) amine groups together (Table S1). Therefore, the degree of ionization is rather low at pH 10 (nearly 5%) (Clark and Hammond, 2000). Moreover, the mass deposition escalates with the incorporation of poorly ionized polymer chains as explained earlier. This results in an overall reduction in the charge density of the multilayer in the bulk of the film at pH 10. Protonated sites of PEI decrease so as do the ion exchange sites. This brings down the rejection percentage of phosphate at pH 10.

The low rejection of phosphate and low negative rejection of chloride causes a decrease in selectivity. For $(PEI/PSS)_9$, the negative rejection of chloride decreases from −301 at pH 4 to −67 at pH 10. For membranes with larger pore size and very high flux, the flux of the ions through the pores is not limited by diffusion. The existence of high surface charge density on the pore walls along with the high flux could result in co-ion exclusion from the membrane surface. In the present case, the PSS top layer and the co-ions Cl^- and $H_2PO_4^-$ bear the same charge which leads to the charge exclusion. The negative rejection of an ion occurs due to a drop in the electric potential across a membrane (termed filtration potential) due to the selective retention of a co-ion (Yaroshchuk, 2008; Mir and Shukla, 2010; Disha et al., 2012; Cheng et al., 2013; Evdochenko et al., 2021). PEI/PSS multilayer is permeable to Na^+, and partially permeable to Cl^- but retains $H_2PO_4^-$. The high permeability of Na^+ creates a positive potential on the permeate side that pulls extra Cl^- to the permeate side by electric migration in addition to the convective flux of Cl^-. A notable fall in negative rejection of Cl^- occurs when deposition pH shifts from 4 to 10. This is due to the reduced rejection of phosphate with pH. At basic pH, PEI assumes less charged layers with loopy conformation during the deposition which leads to thicker film with smaller pores. This could be partially contributing to the reduction in negative solute rejection with the increase in deposition pH. This argument is supported by the permeability values given in Table S2. Flux and hence permeability reduce considerably for each bilayer with the increase in deposition pH. SEM images presented in Fig. 1b also indicate larger mass gain and a lesser number of pores distributed at deposition pH 10. The decrease in percentage flux at 0.15 M and 0.5 M NaCl as presented in Fig. S7 also complies with the above arguments. The reduction in the number of pores and less charge density on the pore walls can be attributed as the possible reasons behind the observed decrease in negative rejection.

3.2.1. $Cl^-/H_2PO_4^-$ permeation characteristics as a function of deposition salt

To see the effect of the ionic strength of polyelectrolyte solution on the anion retention, each bilayer was constructed in 0–0.5 M NaCl. The corresponding percentage rejection and selectivity values are given in Table S4 and Table S5. The percentage rejection of $H_2PO_4^-$ increases from 36 for $(PEI/PSS)_6$ to 45 for $(PEI/PSS)_9$ for zero added salt. The percentage rejection without any deposition salt is higher at the low ionized state of PEI (pH 10) in comparison to the higher ionized state (32% rejection for $(PEI/PSS)_9$ at pH 5.4) (Disha et al., 2012). This is quite reasonable since a thicker coating is formed here as inferred from the thickness (Fig. 4) and permeability values presented in Table S2. The variation of ionic strength at pH 10 does not significantly influence the retention of $H_2PO_4^-$. The increase in ionic strength from 0 to 0.5 M increases the percentage rejection of $H_2PO_4^-$ only by 10%. The low ionized state of PEI seems to provide a poor separation window for $Cl^-/H_2PO_4^-$ through PEI/PSS multilayers. At deposition pH 6, a similar increment in ionic strength (0–0.5 M NaCl) increased the percentage rejection of $H_2PO_4^-$ up to 60–70%. The transport profile at pH 8 (Table S5) follows the same trend as pH 6. These results show that extrinsic compensation is very less at pH 10, Donnan exclusion is not the major mechanism, and rejection of $H_2PO_4^-$ takes place by the affinity of the large amount of weakly ionized PEI towards $H_2PO_4^-$. Furthermore, the affinity can be accounted for in terms of H-bonding and electrostatic forces operated between PEI and phosphate ion (Birnbaum et al., 2003). The lower negative solute rejection values of Cl^- at basic pH also imply that fewer ion exchange sites are present when compared to acidic pH. This points out that the ion exchange mechanism appears to have only a minor role at pH 10. The relative rejection of phosphate at pH 6 to that at pH 10 (Table S6) clearly demonstrates that the rejection of phosphate and hence the ion exchange capacity of PEI/PSS multilayer film at pH 6 is much higher than pH 10 and this effect is more evident at higher deposition salt concentrations. The $Cl^-/H_2PO_4^-$ selective separation window is very narrow at higher pH except in the absence of salt in the deposition medium. This substantiates the establishment of non-electrostatic interactions at pH 10 and electrostatic interactions at pH 6. At acidic deposition pH the normal trend of flux decline with the increase in the number of layers is followed whereas, at basic deposition pH at 0.15 M deposition salt, the flux decline is not evident due to the thinner layers. On the other hand, the flux decline is noticeable at 0.5 M deposition salt affirming the increment in thickness. The selectivity and flux of the PEI/PSS multilayer discussed in the present study are compared with the anion selectivity and flux of various polyelectrolyte

multilayer membranes discussed in the literature (Table S9). The performance of the PEI/PSS membrane for anion removal is comparable with the performance reported in the literature.

3.3. OXY permeation characteristics of PEI/PSS films assembled by hydrophobic interactions at pH 10

The anion filtration study demonstrates that anion retention is higher with PEI/PSS multilayer deposited using electrostatic interactions (acidic pH, highly charged PE) and that is lower with multilayer deposited using non-electrostatic interactions (pH 10, weakly charged PE). So, the multilayer deposited at pH 10 using non-electrostatic (hydrophobic) interactions may be capable of removing hydrophobic uncharged solutes. With this view, the removal of OXY, a widely used UV-filter identified as an emergent contaminant worldwide (DiNardo and Downs, 2018), was analyzed using PEI/PSS multilayer. OXY is a hydrophobic benzophenone derivative with a relatively high log K_{ow} value of 3.6 (properties given in Table S7). PEI/PSS multilayer deposited at pH 10 at 0.15 M NaCl which shows the highest hydrophobicity (Fig. S6) was evaluated for the retention of OXY.

Control filtrations were performed with pristine Nylon 6,6 support membranes of 0.45 μm pore size. Batch mode filtrations consisting of several cycles were performed using a single membrane to evaluate the nature of adsorption. A batch consisted of seven cycles throughout which a constant feed volume was maintained by supplementing additional feed solution (10 mg/L solutions of OXY). The permeation characteristics were monitored in between each cycle (Table 2). The OXY retention by the pristine support membranes was found to be decreasing with each cycle. During the first cycle, the membrane was able to retain 63% of OXY which steadily decreased up to 9% during 7th cycle. The flux was decreased from 6332 L $m^{-2}{\cdot}h^{-1}$ to 5416 L $m^{-2}{\cdot}h^{-1}$. The retention of OXY during the first cycle could be due to the adsorption of OXY to the Nylon 6,6 support by hydrogen bonding and weak electrostatic interactions. When the interactive sites of the pristine membrane are saturated, the retention drops drastically.

PEI/PSS multilayer membrane deposited at pH 10 at 0.15 M NaCl showed a rejection of more than 90% for up to three cycles (Table S8). The percentage rejection remained 86% even at the end of 7th cycle (Table 2). The flux was decreased from 6416 L $m^{-2}{\cdot}h^{-1}$ to 6124 L $m^{-2}{\cdot}h^{-1}$. The hydrophobic interactions between OXY and the multilayer surface have enabled high adsorption of OXY on the surface. Many such hydrophobic organic solutes can undergo adsorption due to hydrogen bonding and hydrophobic interactions (Yangali-Quintanilla et al., 2009). The surface roughness produced by the adsorption of OXY during initial filtration could have facilitated further adsorption. At the same time, the slight decrease in rejection during consecutive filtrations is probably due to the diffusion of solute from the saturated sites of adsorption (Yangali-Quintanilla et al., 2009). Unlike the unmodified support, the PEI/PSS multilayer membranes do not show a sharp decline in flux. This is likely due to the retention of porosity, even after the adsorption of OXY.

Table 2
The % rejection of OXY (10 mg/L) in presence of Cl^-, SO_4^{2-} and NO_3^- (50 mg/L) and SDS (0.05–1.0 CMC) by $(PEI/PSS)_5$ modified MF deposited at 0.15 M NaCl, pH 10.

Batch	$(PEI/PSS)_n$	% OXY Rejection[a]						
		No ions (control)	Anions (50 mg/L)			SDS (CMC)		
			Cl^-	SO_4^{2-}	NO_3^-	0.05	0.5	1.0
1st cycle	pristine	63	94	90	53	99	92	20
	$(PEI/PSS)_5$	94	92	90	94	96	98	96
7th cycle	pristine	9	3	8	2	20	9	1
	$(PEI/PSS)_5$	86	11	33	9	7	3	5

[a] Error $\leq \pm$ 4 %, pristine = unmodified Nylon 6, 6.

3.4. Effect of inorganic ions and surfactant on the rejection of OXY

The presence of anions may interfere OXY removal if the mechanism of removal by PEI/PSS multilayer is charge interaction dominated. On the other hand, the presence of surfactants may interfere OXY removal if the removal mechanism is hydrophobic interaction dominated. Therefore, OXY removal was evaluated in presence of 50 mg/L of chloride, sulphate and nitrate. For the pristine support, the rejection of OXY increased in the presence of Cl^- and SO_4^{2-} ions but decreased in the presence of NO_3^- ions during the first cycle. However, during the 7th cycle, the presence of Cl^- and NO_3^- ions lower the rejection of OXY whereas SO_4^{2-} ions do not interfere with the rejection considerably. In the case of PEI/PSS modified membranes, NO_3^- and Cl^- do not interfere with the rejection of OXY during the first cycle whereas, SO_4^{2-} ions reduce the rejection slightly. As the OXY rejection is not considerably altered by the anions, it can be inferred that charge interaction between OXY and the PEI/PSS multilayer is not the major mechanism of removal.

The interference of ions on the rejection of OXY is prominent towards the final cycle of filtrations. The difference in rejection trends across different ions can be explained based on the Hofmeister series. The Hofmeister series lines up the relative specific ion effects that influence the physical behavior of a wide variety of aqueous processes. The typical order of the anion series is $CO_3^{2-} > SO_4^{2-} > H_2PO_4^- > F^- > Cl^- > Br^- > NO_3^- > I^- > ClO_4^- > SCN^-$ (Kunz et al., 2004; Zhang and Cremer, 2006). The ions to the left of Cl^- are called kosmotropes, while those to its right are called chaotropes. Small or multiply charged kosmotropic ions interfere strongly with local water hydrogen bonding and are strongly hydrated. This gives rise to stabilizing and salting-out effects on proteins and macromolecules (Zhang et al., 2005). On the other hand, large singly charged chaotropic ions seem to correlate with a low charge density and they have smaller effects on the local hydrogen bonding. They usually give rise to salting in behavior which is observed as the denaturation of folded proteins. In the case of OXY, in presence of the kosmotropic SO_4^{2-} ions and Cl^- ions, higher rejection is observed for the overall cycles (Table S8). This could be due to the salting out effects of the ions which leads to the aggregation of OXY that facilitate its exclusion upon filtration. In contrast, the presence of chaotropic NO_3^- ions facilitates the salting-in of OXY, which does not induce aggregation.

On the other hand, the presence of surfactant enhanced the OXY removal in the first cycle at all surfactant concentrations. This indicates that OXY removal by PEI/PSS could be based on hydrophobic interactions. Surfactants can form large aggregates with the hydrophobic solutes that could be easily removed upon filtration. When the surfactants are added above the critical micelle concentration (CMC) to the contaminated water, the surfactant monomers assemble to form micelles within which the contaminants may get solubilized. Thus, the contaminant-trapped aggregates are formed with a larger diameter. The presence of SDS increases rejection of OXY at CMC of 0.05 and 0.5 whereas it reduces at 1.0. The presence of SDS reduces the rejection at higher cycles, especially for a higher concentration of surfactant. With PEI/PSS modified membranes also, the presence of the surfactant essentially reduces the rejection of OXY.

The CMC of SDS is 8.2 mM. At lower concentrations, the SDS exists with a hydrophilic sulphate head and hydrophobic 12-carbon tail. During the filtration of OXY containing a low concentration of SDS, the hydrophobic tail of SDS could engage in interaction with the hydrophobic multilayer surface. The hydrophobic tail attaches to the surface and the hydrophilic anionic head projects to the bulk of the feed solution. The electrostatic repulsion presented by this polar head to OXY with a high polar surface area offers some resistance to its permeation during initial filtration. Yet, the masking of the multilayer surface by the surfactant hinders the interaction of OXY and the surface, which decreases the rejection of OXY in consecutive cycles. At high surfactant concentrations, the formed micelles close the hydrophobic domains of

OXY in it, thus again reducing the hydrophobic interaction of OXY with the surface. Even though the size of the solute increase by micellization, the outer hydrophilic domains facilitate the diffusion of OXY through the membrane, which causes poor rejection of it at high surfactant concentration.

By and large, the contribution of buildup interactions of PEI/PSS polyelectrolyte under different ionic strengths and pHs to the removal of both ionic and non-ionic solutes is demonstrated for the first time. The anionic removal efficiency and permeability values observed in the present filtration at low deposition pH are comparable or even superior to many of the reported polyelectrolyte multilayer membrane filtration (Table S9). The polyelectrolyte multilayer deposited at pH 10 produces membranes suitable for the removal of a hydrophobic non-ionic solute such as OXY. During the batch process, the multilayer coated membrane provides a consistent micropollutant removal when compared to the unmodified support membrane. Therefore, the PEI/PSS multilayer system demonstrates to be a suitable candidate for the removal of micropollutants and anions encountered in water. The usage of PEI/PSS multilayer membranes is limited by the fact that they are better suited for customized applications to remove certain contaminants, and a single module may not remove the complete spectrum of pollutants. Thus, this study also demonstrates that the buildup interactions driving the multilayer assembly have to be carefully chosen depending on the required application of the PEM membrane.

4. Conclusion

The physico-chemical properties of an LbL-assembled PEM membrane depend greatly on the multilayer assembly conditions. Very careful control over deposition parameters can establish a highly selective multilayered membrane for the treatment of wastewater having specific pollutants. Here we evaluated the influence of deposition pH and ionic strength on buildup interactions that determine the growth of multilayer over a polymer membrane. An in-depth understanding of interactions of polyions with each other and with counter ions at their low (pH 10) and high (pH 4–6) ionized state is obtained. The shifting of polyelectrolyte electrostatic interactions to non-electrostatic interactions at acidic and alkaline pHs under different ionic strengths controls the ionic and non-ionic solute transport behavior of the multilayer. The surface of the membrane deposited at acidic pH 4–6 due to the electrostatic interactions of the polyelectrolytes is enriched with plenty of charged sites resulting in good phosphate recovery and anion selectivity ($Cl^-/H_2PO_4^-$ selectivity of 245 at pH 4 and 310 at pH 5.4). Whereas the multilayer membrane deposited at pH 10 due to the non-electrostatic (hydrophobic) interactions is found to be more suitable for the separation of non-ionic solutes (up to 98% rejection of OXY in presence of surfactant). The observations highlight the importance of the polyelectrolyte multilayer buildup interactions to control the membrane properties such as wettability, thickness and internal structure.

Declaration of competing interest

The authors declare that they have no known competing financial interests or personal relationships that could have appeared to influence the work reported in this paper.

Data availability

Data will be made available on request.

Acknowledgments

Sophisticated Analytical Instrument Facilities (SAIF)- Department of Science and Technology (DST) of Mahatma Gandhi University, Kottayam is thanked for providing AFM facility.

Appendix A. Supplementary data

Supplementary data to this article can be found online at https://doi.org/10.1016/j.chemosphere.2023.141078.

References

Abtahi, S.M., Ilyas, S., Joannis Cassan, C., Albasi, C., de Vos, W.M., 2018. Micropollutants removal from secondary-treated municipal wastewater using weak polyelectrolyte multilayer based nanofiltration membranes. J. Membr. Sci. 548, 654–666.

Aravind, U.K., Mathew, J., Aravindakumar, C.T., 2007. Transport studies of BSA, lysozyme and ovalbumin through chitosan/polystyrene sulfonate multilayer membrane. J. Membr. Sci. 299, 146–155.

Athullya, M.K., Dineep, D., Mathew, M.L., Aravindakumar, C.T., Aravind, U.K., 2022. Identification of micropollutants from graywater of different complexity and remediation using multilayered membranes. Environ. Sci. Pollut. Res. 29, 4206–4218.

Bellona, C., Drewes, J.E., Xu, P., Amy, G., 2004. Factors affecting the rejection of organic solutes during NF/RO treatment—a literature review. Water Res. 38, 2795–2809.

Birnbaum, E.R., Rau, K.C., Sauer, N.N., 2003. Selective anion bBinding from water using soluble polymers. Separ. Sci. Technol. 38, 389–404.

Bogdan, A., Robles Aguilar, A.A., Michels, E., Meers, E., 2020. Municipal wastewater as a source for phosphorus. In: Meers, E., Velthof, G., Michels, E., Rietra, R. (Eds.), Biorefinery of Inorganics: Recovering Mineral Nutrients from Biomass and Organic Waste. John Wiley & Sons Ltd, Hoboken, USA, pp. 83–94.

Bóna, Á., Galambos, I., Nemestóthy, N., 2023. Progress towards stable and high-performance polyelectrolyte multilayer nanofiltration membranes for future wastewater treatment applications. Membranes 13, 368.

Cerozi, B.d.S., Fitzsimmons, K., 2016. The effect of pH on phosphorus availability and speciation in an aquaponics nutrient solution. Bioresour. Technol. 219, 778–781.

Chen, J., Xu, S., Tang, C.Y., Hu, B., Tokay, B., He, T., 2023. Stability of layer-by-layer nanofiltration membranes in highly saline streams. Desalination 555, 116520.

Cheng, C., Yaroshchuk, A., Bruening, M.L., 2013. Fundamentals of selective ion transport through multilayer polyelectrolyte membranes. Langmuir 29, 1885–1892.

Cheng, W., Liu, C., Tong, T., Epsztein, R., Sun, M., Verduzco, R., Ma, J., Elimelech, M., 2018. Selective removal of divalent cations by polyelectrolyte multilayer nanofiltration membrane: role of polyelectrolyte charge, ion size, and ionic strength. J. Membr. Sci. 559, 98–106.

Choi, J., Rubner, M.F., 2005. Influence of the degree of ionization on weak polyelectrolyte multilayer assembly. Macromolecules 38, 116–124.

Clark, S.L., Hammond, P.T., 2000. The role of secondary interactions in selective electrostatic multilayer deposition. Langmuir 16, 10206–10214.

Cochin, D., Passmann, M., Wilbert, G., Zentel, R., Wischerhoff, E., Laschewsky, A., 1997. Layered nanostructures with LC-polymers, polyelectrolytes, and inorganics. Macromolecules 30, 4775–4779.

Copley, R.R., Barton, G.J., 1994. A structural analysis of phosphate and sulphate binding sites in proteins: estimation of propensities for binding and conservation of phosphate binding sites. J. Mol. Biol. 242, 321–329.

Decher, G., Schlenoff, J.B., 2003. Multilayer Thin Films- Sequential Assembly of Nanocomposite Materials. Wiley-VCH, Weinheim, Germany.

Devaisy, S., Kandasamy, J., Nguyen, T.V., Johir, M.A.H., Ratnaweera, H., Vigneswaran, S., 2022. Comparison of membrane-based treatment methods for the removal of micro-pollutants from reclaimed water. Water 14, 3708.

DiNardo, J.C., Downs, C.A., 2018. Dermatological and environmental toxicological impact of the sunscreen ingredient oxybenzone/benzophenone-3. J. Cosmet. Dermatol. 17, 15–19.

Disha, V.J., Aravindakumar, C.T., Aravind, U.K., 2012. Phosphate recovery by high flux low pressure multilayer membranes. Langmuir 28, 12744–12752.

Dong, C., He, R., Xu, S., He, H., Chen, H., Zhang, Y.-B., He, T., 2022. Layer-by-layer (LBL) hollow fiber nanofiltration membranes for seawater treatment: ion rejection. Desalination 534, 115793.

Downs, C.A., Bishop, E., Diaz-Cruz, M.S., Haghshenas, S.A., Stien, D., Rodrigues, A.M.S., Woodley, C.M., Sunyer-Caldú, A., Doust, S.N., Espero, W., Ward, G., Farhangmehr, A., Tabatabaee Samimi, S.M., Risk, M.J., Lebaron, P., DiNardo, J.C., 2022. Oxybenzone contamination from sunscreen pollution and its ecological threat to Hanauma Bay, Oahu, Hawaii, U.S.A. Chemosphere 291, 132880.

Dubas, S.T., Schlenoff, J.B., 1999. Factors controlling the growth of polyelectrolyte multilayers. Macromolecules 32, 8153–8160.

Durmaz, E.N., Sahin, S., Virga, E., de Beer, S., de Smet, L.C.P.M., de Vos, W.M., 2021. Polyelectrolytes as building blocks for next-generation membranes with advanced functionalities. ACS Appl. Polym. Mater. 3, 4347–4374.

Elzbieciak, M., Zapotoczny, S., Nowak, P., Krastev, R., Nowakowska, M., Warszyński, P., 2009. Influence of pH on the structure of multilayer films composed of strong and weak polyelectrolytes. Langmuir 25, 3255–3259.

Enault, J., Loret, J.-F., Neale, P.A., de Baat, M.L., Escher, B.I., Belhadj, F., Kools, S.A.E., Pronk, G.J., Leusch, F.D.L., 2023. How effective are water treatment processes in removing toxic effects of micropollutants? A literature review of effect-based monitoring data. J. Water Health 21, 235–250.

Evdochenko, E., Kamp, J., Dunkel, R., Nikonenko, V.V., Wessling, M., 2021. Charge distribution in polyelectrolyte multilayer nanofiltration membranes affects ion separation and scaling propensity. J. Membr. Sci. 636, 119533.

Fu, J., Schlenoff, J.B., 2016. Driving forces for oppositely charged polyion association in aqueous solutions: enthalpic, entropic, but not electrostatic. J. Am. Chem. Soc. 138, 980–990.
Gavrila, A.A., Dasteridis, I.S., Tzimas, A.A., Chatzimitakos, T.G., Stalikas, C.D., 2023. Benzophenones in the environment: Occurrence, fate and sample preparation in the analysis. Molecules 28, 1229.
Ghiorghita, C.-A., Mihai, M., 2021. Recent developments in layer-by-layer assembled systems application in water purification. Chemosphere 270, 129477.
Gopalakrishnan, A., Mathew, M.L., Chandran, J., Winglee, J., Badireddy, A.R., Wiesner, M., Aravindakumar, C.T., Aravind, U.K., 2015. Sustainable polyelectrolyte multilayer surfaces: Possible matrix for salt/dye separation. ACS Appl. Mater. Interfaces 7, 3699–3707.
Guo, H., Ma, Y., Sun, P., Cui, S., Qin, Z., Liang, Y., 2015. Self-cleaning and antifouling nanofiltration membranes—superhydrophilic multilayered polyelectrolyte/CSH composite films towards rejection of dyes. RSC Adv. 5, 63429–63438.
Guyomard, A., Muller, G., Glinel, K., 2005. Buildup of Multilayers Based on Amphiphilic Polyelectrolytes. Macromolecules 38, 5737–5742.
Guzmán, E., Ritacco, H., Rubio, J.E.F., Rubio, R.G., Ortega, F., 2009. Salt-induced changes in the growth of polyelectrolyte layers of poly(diallyl-dimethylammonium chloride) and poly(4-styrene sulfonate of sodium). Soft Matter 5, 2130–2142.
Guzmán, E., Rubio, R.G., Ortega, F., 2020. A closer physico-chemical look to the Layer-by-Layer electrostatic self-assembly of polyelectrolyte multilayers. Adv. Colloid Interface Sci. 282, 102197.
Hasan, M.N., Altaf, M.M., Khan, N.A., Khan, A.H., Khan, A.A., Ahmed, S., Kumar, P.S., Naushad, M., Rajapaksha, A.U., Iqbal, J., Tirth, V., Islam, S., 2021. Recent technologies for nutrient removal and recovery from wastewaters: A review. Chemosphere 277, 130328.
Hong, S.U., Miller, M.D., Bruening, M.L., 2006. Removal of Dyes, Sugars, and Amino Acids from NaCl Solutions Using Multilayer Polyelectrolyte Nanofiltration Membranes. Ind. Eng. Chem. Res. 45, 6284–6288.
Itano, K., Choi, J., Rubner, M.F., 2005. Mechanism of the pH-induced discontinuous swelling/deswelling transitions of poly(allylamine hydrochloride)-containing polyelectrolyte multilayer films. Macromolecules 38, 3450–3460.
Joseph, N., Ahmadiannamini, P., Hoogenboom, R., Vankelecom, I.F.J., 2014. Layer-by-layer preparation of polyelectrolyte multilayer membranes for separation. Polym. Chem. 5, 1817–1831.
Katibi, K.K., Yunos, K.F., Che Man, H., Aris, A.Z., bin Mohd Nor, M.Z., binti Azis, R.S., 2021. Recent advances in the rejection of endocrine-disrupting compounds from water using membrane and membrane bioreactor technologies: A review. Polymers 13, 392.
Khanzada, N.K., Farid, M.U., Kharraz, J.A., Choi, J., Tang, C.Y., Nghiem, L.D., Jang, A., An, A.K., 2020. Removal of organic micropollutants using advanced membrane-based water and wastewater treatment: A review. J. Membr. Sci. 598, 117672.
Kim, S., Park, Y.H., Choi, Y.-E., 2022. Amination of non-functional polyvinyl chloride polymer using polyethyleneimine for removal of phosphorus from aqueous solution. Polymers 14, 1645.
Kim, S., Park, Y.H., Lee, J.B., Kim, H.S., Choi, Y.-E., 2020. Phosphorus adsorption behavior of industrial waste biomass-based adsorbent, esterified polyethylenimine-coated polysulfone-Escherichia coli biomass composite fibers in aqueous solution. J. Hazard Mater. 400, 123217.
Kolasińska, M., Krastev, R., Warszyński, P., 2007. Characteristics of polyelectrolyte multilayers: Effect of PEI anchoring layer and posttreatment after deposition. J. Colloid Interface Sci. 305, 46–56.
Korzhova, E., Déon, S., Koubaa, Z., Fievet, P., Lopatin, D., Baranov, O., 2020. Modification of commercial UF membranes by electrospray deposition of polymers for tailoring physicochemical properties and enhancing filtration performances. J. Membr. Sci. 598, 117805.
Kotov, N.A., 1999. Layer-by-layer self-assembly: The contribution of hydrophobic interactions. Nanostruct. Mater. 12, 789–796.
Kovacevic, D., van der Burgh, S., de Keizer, A., Cohen Stuart, M.A., 2002. Kinetics of formation and dissolution of weak polyelectrolyte multilayers: Role of salt and free polyions. Langmuir 18, 5607–5612.
Kunz, W., Henle, J., Ninham, B.W., 2004. 'Zur Lehre von der Wirkung der Salze' (about the science of the effect of salts): Franz Hofmeister's historical papers. Curr. Opin. Colloid Interface Sci. 9, 19–37.
Lorena Cortez, M., De Matteis, N., Ceolín, M., Knoll, W., Battaglini, F., Azzaroni, O., 2014. Hydrophobic interactions leading to a complex interplay between bioelectrocatalytic properties and multilayer meso-organization in layer-by-layer assemblies. Phys. Chem. Chem. Phys. 16, 20844–20855.
Lösche, M., Schmitt, J., Decher, G., Bouwman, W.G., Kjaer, K., 1998. Detailed structure of molecularly thin polyelectrolyte multilayer films on solid substrates as revealed by neutron reflectometry. Macromolecules 31, 8893–8906.
Lu, Y., Wu, Y., Liang, J., Libera, M.R., Sukhishvili, S.A., 2015. Self-defensive antibacterial layer-by-layer hydrogel coatings with pH-triggered hydrophobicity. Biomaterials 45, 64–71.
Luo, Y., Guo, W., Ngo, H.H., Nghiem, L.D., Hai, F.I., Zhang, J., Liang, S., Wang, X.C., 2014. A review on the occurrence of micropollutants in the aquatic environment and their fate and removal during wastewater treatment. Sci. Total Environ. 473–474, 619–641.
Lvov, Y., Ariga, K., Ichinose, I., Kunitake, T., 1995. Assembly of multicomponent protein films by means of electrostatic layer-by-layer adsorption. J. Am. Chem. Soc. 117, 6117–6123.
Mathew, J., Gopalakrishnan, A., Aravindakumar, C.T., Aravind, U.K., 2017. Transport properties and morphology of CHI/PSS multilayered microfiltration membranes for the low pressure filtration of amino acids. J. Chem. Technol. Biotechnol. 92, 834–844.
Mir, F.Q., Shukla, A., 2010. Negative rejection of NaCl in ultrafiltration of aqueous solution of NaCl and KCl using sodalite octahydrate zeolite−clay charged ultrafiltration membrane. Ind. Eng. Chem. Res. 49, 6539–6546.
Mohamad, H.S., Neuber, S., Helm, C.A., 2019. Surface forces of asymmetrically grown polyelectrolyte multilayers: searching for the charges. Langmuir 35, 15491–15499.
Nazaran, P., Bosio, V., Jaeger, W., Anghel, D.F., von Klitzing, R., 2007. Lateral mobility of polyelectrolyte chains in multilayers. J. Phys. Chem. B 111, 8572–8581.
Nestler, P., Block, S., Helm, C.A., 2012. Temperature-induced transition from odd–even to even–odd effect in polyelectrolyte multilayers due to interpolyelectrolyte interactions. J. Phys. Chem. B 116, 1234–1243.
Ogawa, K., 2015. Effects of salt on intermolecular polyelectrolyte complexes formation between cationic microgel and polyanion. Adv. Colloid Interface Sci. 226, 115–121.
Ojajuni, O., Saroj, D., Cavalli, G., 2015. Removal of organic micropollutants using membrane-assisted processes: a review of recent progress. Environmental Technology Reviews 4, 17–37.
Ou, Z., Muthukumar, M., 2006. Entropy and enthalpy of polyelectrolyte complexation: Langevin dynamics simulations. J. Chem. Phys. 124, 154902.
Ouyang, L., Malaisamy, R., Bruening, M.L., 2008. Multilayer polyelectrolyte films as nanofiltration membranes for separating monovalent and divalent cations. J. Membr. Sci. 310, 76–84.
Pap, S., Zhang, H., Bogdan, A., Elsby, D.T., Gibb, S.W., Bremner, B., Taggart, M.A., 2023. Pilot-scale phosphate recovery from wastewater to create a fertiliser product: An integrated assessment of adsorbent performance and quality. Water Res. 228, 119369.
Peng, C., Thio, Y.S., Gerhardt, R.A., 2012. Effect of precursor-layer surface charge on the layer-by-layer assembly of polyelectrolyte/nanoparticle multilayers. Langmuir 28, 84–91.
Rathee, V.S., Sidky, H., Sikora, B.J., Whitmer, J.K., 2018. Role of associative charging in the entropy–energy balance of polyelectrolyte complexes. J. Am. Chem. Soc. 140, 15319–15328.
Ruths, J., Essler, F., Decher, G., Riegler, H., 2000. Polyelectrolytes I: Polyanion/polycation multilayers at the air/monolayer/water interface as elements for quantitative polymer adsorption studies and preparation of hetero-superlattices on solid surfaces. Langmuir 16, 8871–8878.
Sanyal, O., Lee, I., 2014. Recent progress in the applications of layer-by-layer assembly to the preparation of nanostructured ion-rejecting water purification membranes. J. Nanosci. Nanotechnol. 14, 2178–2189.
Saqib, J., Aljundi, I.H., 2016. Membrane fouling and modification using surface treatment and layer-by-layer assembly of polyelectrolytes: State-of-the-art review. J. Water Process Eng. 11, 68–87.
Sasi, S., Rayaroth, M.P., Aravindakumar, C.T., Aravind, U.K., 2020. Occurrence, distribution and removal of organic micro-pollutants in a low saline water body. Sci. Total Environ. 749, 141319.
Scheele, A., Sutter, K., Karatum, O., Danley-Thomson, A.A., Redfern, L.K., 2023. Environmental impacts of the ultraviolet filter oxybenzone. Sci. Total Environ. 863, 160966.
Schlenoff, J.B., Rmaile, A.H., Bucur, C.B., 2008. Hydration contributions to association in polyelectrolyte multilayers and complexes: Visualizing hydrophobicity. J. Am. Chem. Soc. 130, 13589–13597.
Schneider, S.L., Lim, H.W., 2019. Review of environmental effects of oxybenzone and other sunscreen active ingredients. J. Am. Acad. Dermatol. 80, 266–271.
Schoeler, B., Kumaraswamy, G., Caruso, F., 2002. Investigation of the influence of polyelectrolyte charge density on the growth of multilayer thin films prepared by the layer-by-layer technique. Macromolecules 35, 889–897.
Shchepelina, O., Drachuk, I., Gupta, M.K., Lin, J., Tsukruk, V.V., 2011. Silk-on-Silk Layer-by-Layer Microcapsules. Adv. Mater. 23, 4655–4660.
Shchukin, D.G., Zheludkevich, M., Yasakau, K., Lamaka, S., Ferreira, M.G.S., Möhwald, H., 2006. Layer-by-layer assembled nanocontainers for self-healing corrosion protection. Adv. Mater. 18, 1672–1678.
Shiratori, S.S., Rubner, M.F., 2000. pH-dependent thickness behavior of sequentially adsorbed layers of weak polyelectrolytes. Macromolecules 33, 4213–4219.
Sukhorukov, G.B., Antipov, A.A., Voigt, A., Donath, E., Möhwald, H., 2001. pH-controlled macromolecule encapsulation in and release from polyelectrolyte multilayer nanocapsules. Macromol. Rapid Commun. 22, 44–46.
Sumi, T., Suzuki, C., Sekino, H., 2009. Hydrophobic effects on multivalent-salt-induced self-condensation of DNA. J. Chem. Phys. 131, 161103.
Thomas, J.M., Aravindakumar, C.T., Aravind, U.K., 2020. Removal of beta blockers using polyelectrolyte monolayered membrane and its antifouling performance. J. Ind. Eng. Chem. 87, 222–233.
Tiourina, O.P., Antipov, A.A., Sukhorukov, G.B., Larionova, N.I., Lvov, Y., Möhwald, H., 2001. Entrapment of α-chymotrypsin into hollow polyelectrolyte microcapsules. Macromol. Biosci. 1, 209–214.
von Klitzing, R., 2006. Internal structure of polyelectrolyte multilayer assemblies. Phys. Chem. Chem. Phys. 8, 5012–5033.
Wang, X., Kim, H.J., Xu, P., Matsumoto, A., Kaplan, D.L., 2005. Biomaterial Coatings by Stepwise Deposition of Silk Fibroin. Langmuir 21, 11335–11341.
Wang, X., Liu, F., Zheng, X., Sun, J., 2011. Water-enabled self-healing of polyelectrolyte multilayer coatings. Angew. Chem. Int. Ed. 50, 11378–11381.
Willner, I., Eichen, Y., Frank, A.J., Fox, M.A., 1993. Photoinduced electron-transfer processes using organized redox-functionalized bipyridinium-polyethylenimine-titania colloids and particulate assemblies. J. Phys. Chem. 97, 7264–7271.
Xanthopoulou, M., Giliopoulos, D., Tzollas, N., Triantafyllidis, K.S., Kostoglou, M., Katsoyiannis, I.A., 2021. Phosphate removal using polyethylenimine functionalized silica-based materials. Sustainability 13, 1502.
Yang, Z., Zhou, Y., Feng, Z., Rui, X., Zhang, T., Zhang, Z., 2019. A review on reverse osmosis and nanofiltration membranes for water purification. Polymers 11, 1252.

Yangali-Quintanilla, V., Sadmani, A., McConville, M., Kennedy, M., Amy, G., 2009. Rejection of pharmaceutically active compounds and endocrine disrupting compounds by clean and fouled nanofiltration membranes. Water Res. 43, 2349–2362.
Yaroshchuk, A.E., 2008. Negative rejection of ions in pressure-driven membrane processes. Adv. Colloid Interface Sci. 139, 150–173.
Zacharia, N.S., Modestino, M., Hammond, P.T., 2007. Factors influencing the interdiffusion of weak polycations in multilayers. Macromolecules 40, 9523–9528.
Zhang, R., Tian, J., Gao, S., Van der Bruggen, B., 2020. How to coordinate the trade-off between water permeability and salt rejection in nanofiltration? J. Mater. Chem. A 8, 8831–8847.
Zhang, X., Xu, Y., Zhang, X., Wu, H., Shen, J., Chen, R., Xiong, Y., Li, J., Guo, S., 2019. Progress on the layer-by-layer assembly of multilayered polymer composites: Strategy, structural control and applications. Prog. Polym. Sci. 89, 76–107.
Zhang, Y., Cremer, P.S., 2006. Interactions between macromolecules and ions: the Hofmeister series. Curr. Opin. Chem. Biol. 10, 658–663.
Zhang, Y., Furyk, S., Bergbreiter, D.E., Cremer, P.S., 2005. Specific Ion Effects on the Water Solubility of Macromolecules: PNIPAM and the Hofmeister Series. J. Am. Chem. Soc. 127, 14505–14510.
Zhao, J., Pan, F., Li, P., Zhao, C., Jiang, Z., Zhang, P., Cao, X., 2013. Fabrication of utrathin membrane via layer-by-layer self-assembly driven by hydrophobic interaction towards high separation performance. ACS Appl. Mater. Interfaces 5, 13275–13283.